11th Australasian Fluid Mechanics Conference
University of Tasmania, Hobart, Australia
14-18 December 1992

MEASUREMENTS IN THE TURBULENT WAKE OF A ROTATING CIRCULAR CYLINDER

D.H. WOOD, P.L. PETERSON and P.D. CLAUSEN

Department of Mechanical Engineering
University of Newcastle, NSW 2308, AUSTRALIA

ABSTRACT

This paper presents mean velocity and Reynolds stress measurements obtained at three axial locations in the turbulent wake of a circular cylinder rotating about the streamwise axis. The ratio of the circumferential velocity of the cylinder to the free-stream axial velocity had a maximum value of 0.6. Measurements for two combinations of axial and circumferential velocities showed that the velocity deficit in the wake was a multi-valued function of the swirl number, implying a complex influence of the rotation on the separation of the cylinder's boundary layer. The rotation eventually removed the negative region in the cross-stream shear stress. This, and other large changes to the turbulence, occurred even though the rotationally-activated generation terms in the Reynolds transport equations never dominated the "non-rotating" terms that also occur in more conventional wakes.

INTRODUCTION

Turbulent flows are often most conveniently analysed using a non-inertial reference frame: important examples include the boundary layers on, and the wakes behind, the rotating blades of propellers, wind turbines and turbomachines. In changing from an inertial to a non-inertial frame, the Navier-Stokes equations gain a fictitious body force consisting of four terms, eg Batchelor (1967, equn 3.2.9). Speziale (1989) has pointed out, however, that only one of these, the Coriolis force, directly influences the fluctuating flow field; any fluid element with a non-zero velocity in the plane of rotation experiences a Coriolis force perpendicular to that velocity. To develop computational models for turbulent transport in non-inertial frames it is necessary, therefore, to study the effects of the Coriolis force on turbulence structure. That is the aim of the work described in this paper. We have documented the response of a well-known flow - the turbulent wake of a circular cylinder - to varying amounts of rotation about the streamwise axis. (For convenience, the unqualified use of the term "rotation" in this paper will imply rotation about the streamwise axis.) The rest of this brief Introduction describes some of the important features of related turbulent flows. The next Section describes the equipment and techniques used to obtain the three mean velocities and six Reynolds stresses. The subsequent Section discusses the results and is followed by the conclusions.

The effect of system rotation on the decay of nominally homogeneous grid-generated turbulence has been studied numerically, Bardina et al. (1985) and experimentally, eg Jacquin et al. (1990). Rotation does not introduce any new terms to the turbulent kinetic equation - which is also the case in the present experiment - but it does reduce the decay of turbulent energy, mainly by inhibiting the spectral transfer of energy from low to high wavenumber. Many measurements have been made on and behind rotating blades, including turbomachinery blades, eg Lakshminarayana (1986), propellers, eg Cenedese et al. (1988), and wind turbines, eg Clausen & Wood (1988). The rotation has a significant effect on the primary shear stress in some of these wakes. For example, fig. 7 of Lakshminarayana (1986) shows no change in sign of the stress across the wake of a compressor blade.

Coriolis accelerations are often associated with streamline curvature, whose effect on nominally plane wakes was studied by Savill (1983), Nakayama (1987) and Weygandt & Mehta (1992). There is a general increase in the turbulence levels on the unstable side and an attenuation on the stable side, Nakayama (1987). Following prolonged curvature, the cross-stream shear stress may lose its negative region, Savill (1983), but this is apparently associated with the disappearance of the region of positive gradient in the mean velocity. The latter occurs for sufficently large differences in streamwise mean velocity across the wake caused, in turn, by the combination of curvature and irrotationality.

EXPERIMENTAL METHODS

Fig. 1 shows the experimental apparatus, whose upstream end was fitted to the outlet of a conventional blower wind tunnel. The co-ordinate system shown in fig. 1 rotates relative to fixed "laboratory" co-ordinates which we will take to be inertial. Mean and fluctuating velocities in the co-ordinate directions are indicated by upper and lower case letters respectively. The swirl generator (with honeycomb to impart the swirl to the air) was used to investigate swirling flow in a conical diffuser, Clausen & Wood (1987), Clausen et al. (1992), and a swirling mixing layer, Mehta et al. (1991) and Wood et al. (1992). All the present results were obtained from an axially-aligned X-probe traversed at a fixed location with the 5 mm circular cylinder at one of the three indicated positions within the rotating part of the swirl generator.

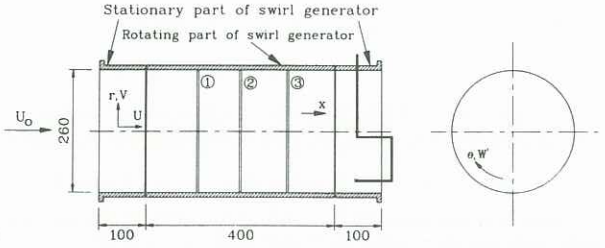

Figure 1. Schematic of cylinder in swirl generator. All dimensions in mm. The numbers indicate the three cylinder locations and the traverse system and probe is indicated at the right.

All probe movement was by stepper motors controlled by a PC-compatible computer that was also fitted with an analogue-to-digital conversion board. Data acquisiton was triggered each time the cylinder passed a particular angular point, which was adjusted to capture as much as possible of the wake at each cylinder location. After triggering, ninety samples were acquired from each wire at a sampling rate of 2.5 kHz. The trigger point was taken as the origin for the circumferential or cross-stream co-ordinate θ. Subsequent values of θ were determined from the sampling rate and Ω, the angular velocity of the swirl generator. All the results were obtained by ensemble averaging over 3,000 revolutions of the swirl generator. This technique of obtaining spatially-dependent information from the time-dependent output of a fixed probe is often called "phase-locked averaging" and further details are given by Clausen & Wood (1988).

The DANTEC 55P51 X-probe was fitted with 5 μm diameter tungsten wires having an active length of 1 mm and copper plated stubs of about 20 μm diameter. The probes were calibrated as described by Clausen & Wood (1989). At each radius the probe was sampled at four roll angles: 0; 45°; 90°; and -45°. Reduction of the data to yield the three mean velocities and six Reynolds stresses was similar to the procedure described in Cutler & Bradshaw (1991); for example, we used the first nine of the equations labelled as equn (1) in that paper.

The rotation or swirl number used to measure the significance of the rotation is defined as $S = \Omega r/U_0$, which is the inverse of the Rossby number. Two combinations of Ω and U_0 were used: 57.6 rad/sec and 19.47 m/sec and 78.5 rad/sec and 13.66 m/sec. For both combinations, profiles were obtained at x = 0.194, 0.294 and 0.394 m so that x/d, where d is the cylinder diameter, varied from 39 to 79. It will be necessary at times to distinguish between the two combinations; this will be done by quoting the value of S_*, defined as S for r = 0.10 m. Nominally, S_* was either 0.29 or 0.58. At each cylinder position and U_0, the wake was also measured with the cylinder stationary, that is, for $S_* = 0$. Some of these results are included in the subsequent figures. For all non-zero values of S_*, measurements were obtained at r = 0.10, 0.08, 0.06 and 0.04 m before a repeat profile was determined at r = 0.10 m. The repeat measurements are shown on the subsequent figures to give an indication of the overall measurement accuracy.

RESULTS AND DISCUSSION

Typical profiles of U/U_0 are shown in fig. 2 for $S_* = 0.58$. Each separate symbol indicates a separate measurement and the (straight) lines without symbols joining successive measurements. The deficit velocity, U_m, does not vary monotonically with radius, implying that the rotation has a complex influence on the separation of the boundary layer on the cylinder. The dependence of U_m on S is shown in fig. 3 for all results. The results tend to collapse on this scaling, except around S = 0.24, suggesting that the rotation has a complex effect on the separation of the cylinder's boundary layer. A similar lack of collapse is evident in the plots of the maximum Reynolds stresses at each radius, such as $\overline{u^2}$ in fig. 4. However, the dependence on S does not follow the dependence of U_m, showing that the latter is not the appropriate velocity scale for normalising the results. Because of this, we have used U_0^2 to normalise all the Reynolds stresses. Fig. 4 also indicates that the rotation does not have a significant effect on the streamwise decay of the turbulence levels.

Only a small fraction of the large amount of Reynolds stress data can be presented here, so we concentrate on the furthest downstream measurements (x = 0.394 m) for the highest S_*. Fig. 5 shows profiles of the axial normal stress,

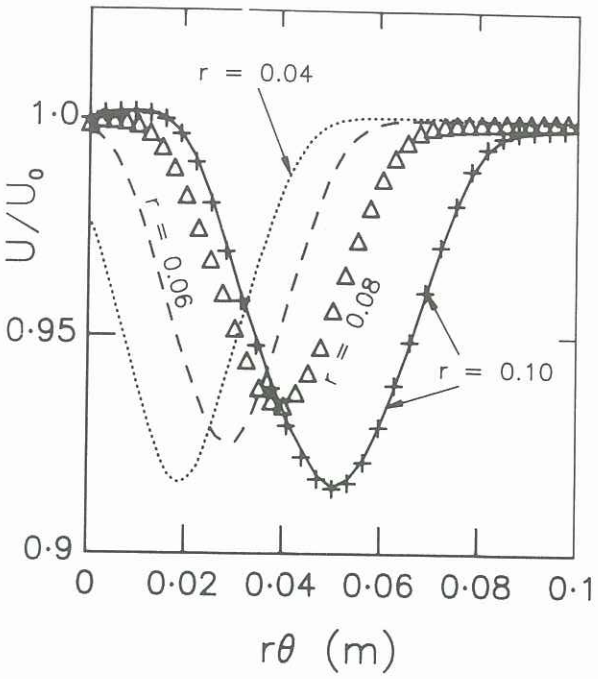

Figure 2. U/U_0 for $S_* = 0.58$ and x = 0.394 m. Radius is indicated on the figure.

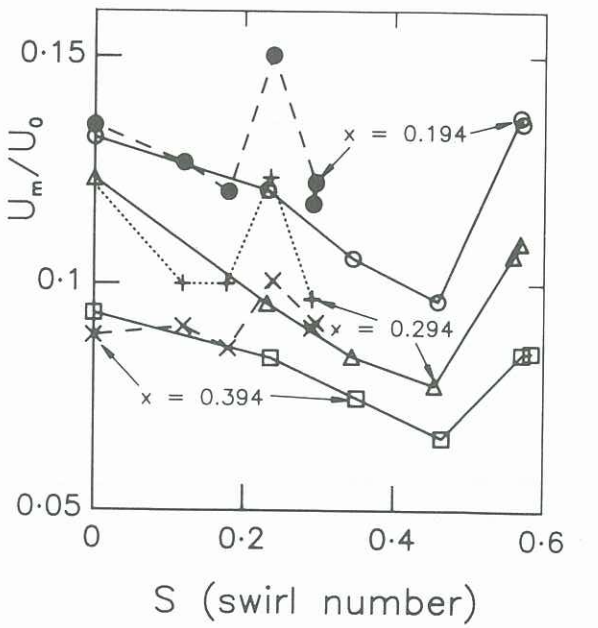

Figure 3. Maximum wake deficit velocity U_m at each radius plotted as a function of swirl number. All results for $S_* = 0.29$ and 0.58 are shown.

$\overline{u^2}$. There is little difference between the results for r = 0.04, 0.06 and 0.08 , but there is a significant increase at r = 0.10. Both $\overline{u^2}$ and $\overline{w^2}$, shown in fig. 6, have pronounced asymmetries, but these tend to cancel when added to give $\overline{q^2}$. Only $\overline{u^2}$ has no Coriolis term in its transport equation but the Coriolis terms in the equations for the other stresses cancel when summed to give the equation for $\overline{q^2}$. The distribution of $\overline{q^2}$ (which is not shown) is remarkably constant for the first three radii but then increases significantly at r = 0.10.

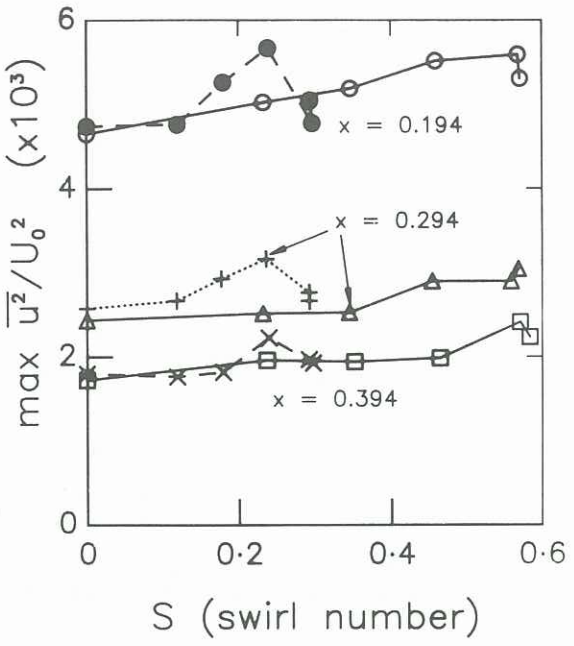

Figure 4. Maximum $\overline{u^2}$ at each radius plotted as a function of swirl number. All results for $S_* = 0.29$ and 0.58 are shown.

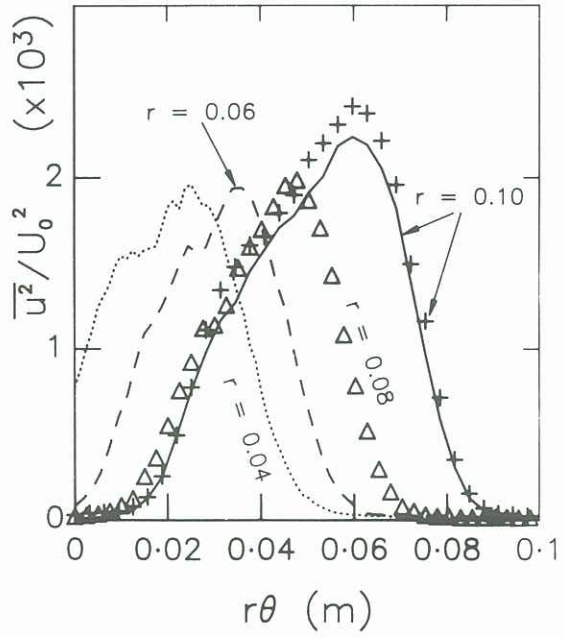

Figure 5. Profiles of $\overline{u^2}$ for $S_* = 0.58$ and $x = 0.394$ m. Radius is indicated on the figure.

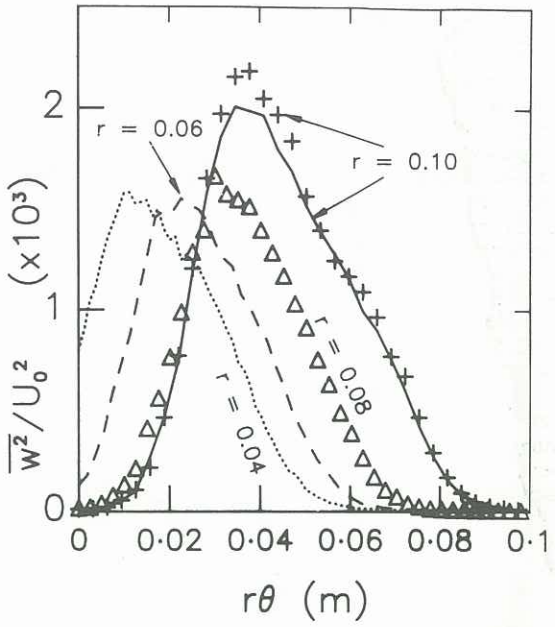

Figure 6. Profiles of $\overline{w^2}$ for $S_* = 0.58$ and $x = 0.394$ m. Radius is indicated on the figure.

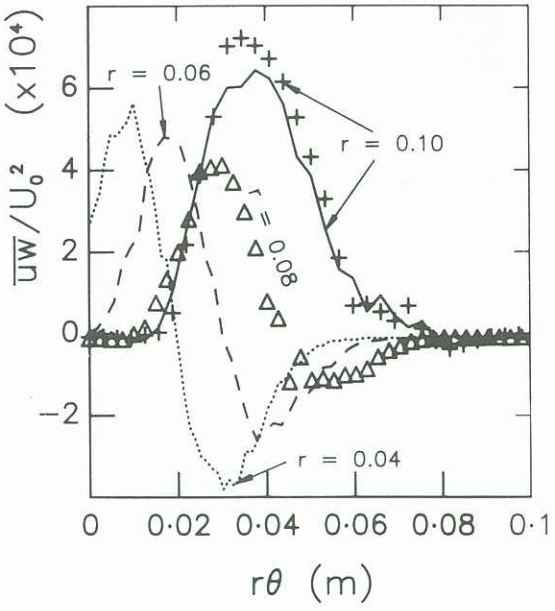

Figure 7. Profiles of $\overline{uw}$ for $S_* = 0.58$ and $x = 0.394$ Radius is indicated on the figure.

The most obvious effect of the rotation on the Reynolds stresses occurs in $\overline{uw}$ which is shown in fig. 7. At small r, $\overline{uw}$ behaves much like it should for S = 0; the positive and negative regions are nearly antisymmetric about the point where $\partial U/\partial z = 0$ and $\overline{uw}$ passes through zero at this point. As S increases, the relative size of the negative region decreases, until at r = 0.10, $\overline{uw}$ is almost everywhere positive. This occurs in spite of $\partial U/\partial r\theta$ being positive for approximately half the wake. A similar behaviour is apparent in fig. 7 of Lakshminarayana (1986) for the wake of a compressor blade. Savill (1983) also found that the equivalent of $\overline{uw}$ in a plane wake became largely positive after prolonged curvature, but this was accompanied by a change in sign of the equivalent to $\partial U/\partial r\theta$. The other shear stresses, $\overline{uv}$ and $\overline{vw}$, are generally smaller in magnitude than $\overline{uw}$.

The main generation terms for $-\overline{uw}$ are shown in fig. 8: these are $-\overline{w^2}\partial U/\partial r\theta$ which is also present in the absence of rotation, and $-2\Omega\overline{uv}$, the Coriolis term . The positive region of the non-rotating term is significantly reduced in magnitude but the net generation remains positive, showing that the positive $\overline{uw}$ is maintained by the non-local terms in the transport equations. A similar conclusion applies to $\overline{u^2}$ as fig. 6 implies that its direct generation, $-\overline{uw}\partial U/\partial r\theta$, is small in the region where $\overline{u^2}$ peaks. In fact, there is a region of "negative

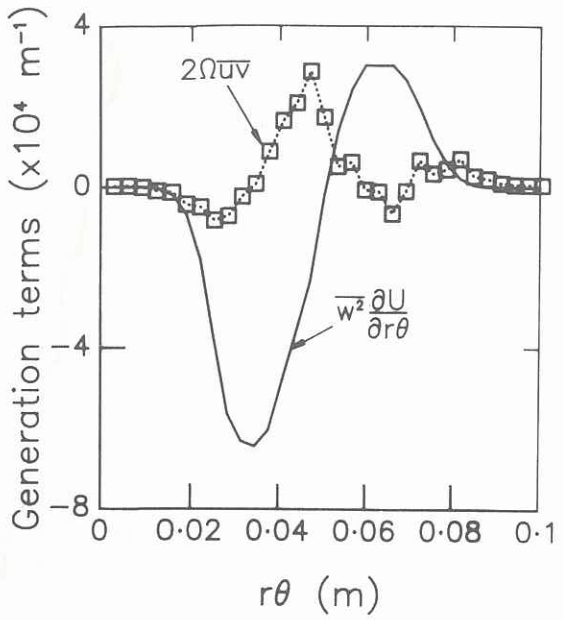

Figure 8. Production terms for $-\overline{uw}$ *at* $S_* = 0.58$, $x = 0.394$ *m and* $r = 0.10$ *m.*

production" of $\overline{u^2}$ around $r\theta = 0.06$. The relative magnitude of the Coriolis term in fig. 7 is typical of all the rotation terms in the Reynolds stress equations in that it never dominates the non-rotating terms.

CONCLUSIONS

The experimental results presented in this paper show that perturbing the wake of a circular cylinder by rotating the cylinder about the streamwise axis causes three major shanges to the wake. Firstly, the deficit velocity at any axial location is a multi-valued function of the swirl number implying that the rotation has a complex effect on the separation of the cylinder's boundary layer. Furthermore, the deficit velocity was not the appropriate scale for normalising the turbulence quantites, which is contrary to the situation in fully-developed, non-rotating wakes. Secondly, the rotation tends to remove the negative region in the cross-stream shear stress without altering the sign of the corresponding mean velocity gradient. Thirdly, the distribution of the generation terms in the Reynolds stress transport equations show that the elevated normal stresses are due largely to the non-local terms in those equations.

These significant changes to the turbulence structure occur without the Coriolis terms dominating the direct generation terms in the transport equations. Somewhat unexpectedly, the rotation did not appear to reduce the streamwise decay of the turbulence levels.

ACKNOWLEDGEMENTS

The work described in this paper was supported by the Australian Research Council.

REFERENCES

BATCHELOR, G.K. (1967). An Introduction to Fluid Dynamics, C.U.P.

BARDINA, J., FERZIGER, J.H. and ROGALLO, R.S. (1985). Effect of rotation on isotropic turbulence: computation and modeling, *J. Fluid Mech.*, **154**, 321 - 336.

CENEDESE, A., ACCARDO, L. and MILONE, R. (1988). Phase sampling in the analysis of a propeller wake, *Expts in Fluids*, **6**, 55 - 60.

CLAUSEN, P.D. and WOOD, D.H. (1987). Some measurements of swirling flow through an axisymmetric diffuser, 6th Symp. Turbulent Shear Flows, Toulouse, France.

CLAUSEN, P.D. and WOOD, D.H. (1988). An experimental investigation of blade element theory for wind turbines. Part 2: phase-locked average results, *J. Wind Eng'g & Ind. Aero.*, **31**, 305 - 322.

CLAUSEN, P.D. and WOOD, D.H. (1989). The correction of X-probe results for transverse contamination, *J. Fluids Eng'g*, **111**, 226 - 228.

CLAUSEN, P.D., KOH, S.G., and WOOD, D.H. (1992). Measurements of a turbulent boundary developing in a conical diffuser, *Exptl Thermal Fluid Sci*, (to appear).

CUTLER, A.D. and BRADSHAW, P. (1991). A crossed hot-wire technique for complex turbulent flows, *Expts in Fluids*, **12**, 17 - 22.

HOFFMANN, P.H., MUCK, K.C. and BRADSHAW, P. (1985).The effect of concave surface curvature on turbulent boundary layers, *J. Fluid Mech.*, **161**, 371 - 397.

JACQUIN, L., LEUCHTER, O., CAMBON, C. and MATHIEU, J. (1990). Homogeneous turbulence in the presence of rotation, *J. Fluid Mech.*, **220**, 1 - 52.

LAKSHMINARAYANA, B. (1986). Turbulence modeling for complex shear flows, *A.I.A.A. J.*, **24**, 1900 - 1917.

MEHTA, R.D., WOOD, D.H., and CLAUSEN, P.D. (1991). Some effects of swirl on turbulent mixing layer development, *Phys. Fluids A*, **3**, 2716 - 2724.

NAKAYAMA, A. (1987). Curvature and pressure-gradient effects on a small-deficit wake, *J. Fluid Mech.*, **175**, 215 - 246.

PLESNIAK, M.W. and JOHNSTON, J.P. (1989). The Effects of Longitudinal Curvature on Turbulent Two-Stream Mixing Layers, Rpt MD-54, Thermosciences Divn, Dept Mechanical Engineering, Stanford University.

SPEZIALE, C.G. (1989). Turbulence modeling in noninertial frames of reference, *Theoret. Comput. Fluid Dynamics*, **1**, 3 - 19.

WYGANDT, J.H. and MEHTA, R.D. (1992). Three-dimensional structure of a curved wake, AIAA Paper 92-0541.

WOOD, D.H., MEHTA, R.D., and KOH, S.G. (1992). Structure of a swirling turbulent mixing layer, *Exptl Thermal Fluid Sci*, **5**, 196 - 202.